Cleaner Engineering and Technology 18 (2024) 100725

Contents lists available at ScienceDirect

Cleaner Engineering and Technology

journal homepage: www.sciencedirect.com/journal/cleaner-engineering-and-technology

Assessment of particulate PAHs toxicity from alcohol-diesel blends fuelled high compression ratio CI engine

Tomesh Kumar Sahu [a], Pravesh Chandra Shukla [a,*], Arindam Mondal [b], Satyajit Gupta [b], Giacomo Belgiorno [c], Gabriele Di Blasio [d]

[a] Department of Mechanical Engineering, Indian Institute of Technology Bhilai, Durg, India
[b] Department of Chemistry, Indian Institute of Technology Bhilai, Durg, India
[c] PUNCH Torino S.p.A., Turin, Italy
[d] Consiglio Nazionale Delle Ricerche - STEMS, Via Marconi, 4, 80125, Naples, Italy

A R T I C L E I N F O

Keywords:
Methanol
Ethanol
Butanol
Particulate morphology
Polycyclic aromatic hydrocarbons
Toxicity equivalent factor

A B S T R A C T

Transport and power generation applications will play an important role in current and next-generation compression ignition (CI) engines. Methanol, ethanol, and butanol have emerged as potential alternative fuels for internal combustion engines capable of reducing overall greenhouse gases (GHG) and pollutant emissions. This study deals with the morphological characterization of particulate matter (PM) and toxicity assessment of polycyclic aromatic hydrocarbons (PAHs) for methanol, ethanol and butanol blending with diesel, and provides new findings and results in the specific literature. It defines new limits of alcohol fractions in diesel blends for their applications in CI engines. For the experimental assessment, a single-cylinder CI engine was used with an increased compression ratio (CR) from 17.5 to 26. Alcohol fraction of 20% (*v/v*) in diesel reduced the PM emissions in the range of 29–38% than diesel. PM was further reduced, up to ~50%, for higher ethanol and butanol fractions (~50%), and the soot morphological characteristics exhibit smaller particle sizes (400–600 nm) than diesel (up to 2 μm). Moreover, 20% of alcohol fraction led to a 34–60% reduction in PAHs. The toxicity evaluation of the tested alcohol-diesel blend indicates that high molecular weight PAHs and *nitro*-PAHs are the main contributors to the overall toxicity. Benzo[a]pyrene and dibenzo-anthracene were the prominent PAHs. Increasing the alcohol blend ratio significantly reduced the toxicity potential, ranging from 20 to 67%.

1. Introduction

Global and local air pollution is one of the major concerns in many countries nowadays. Mitigation and stricter emission norms are being implemented across countries to control pollution and CO_2 emissions from the transportation sector (Joshi, 2023; Ribeiro et al., 2022; Singh et al., 2023). Alternative fuels, such as methanol, ethanol, and butanol play a significant role in minimising these emissions and CO_2, especially for spark ignition (SI) engines, due to their favourable fuel characteristics (octane number, vaporization behaviour, density, etc.) (Sahu et al., 2022a; Tuner, 2016; Verhelst et al., 2019). Alcohol fuels are economically and environmentally friendly if produced locally and from renewable bio-based resources (Yuan et al., 2018; Sahu et al., 2022b). Higher fractions of alcohol in diesel make it difficult to autoignite and to keep stable combustion due to higher autoignition temperature than diesel, limiting their use in compression ignition (CI) engines. Pre-heating the inlet air or increasing the compression ratio (CR) beyond 25:1 are viable strategies to autoignite higher fractions of alcohols in diesel (Sahu et al., 2022a; Shamun et al., 2017). Phase separation phenomenon is an issue for alcohol-diesel blends when it interact with ambient air as it tends to absorb moisture. This leads to the separation of alcohol from diesel, which is undesirable for fuel injection systems (Shanmugam et al., 2021; Lei et al., 2012) as it may lead to unstable combustion. Additives or solubilizers such as oleic acid, dodecanol, etc., are preferable (Shanmugam et al., 2021; Singh and Bharj, 2019) for higher fractions of alcohol-diesel blends to avoid phase separation.

Small-displacement CI engines are widely used as power generators due to the lower total cost of ownership especially for agricultural applications. Most of these engines lack state-of-the-art combustion systems, operating with mechanical fuel injection systems, and without aftertreatment devices. Efficiencies and emissions like particulate matter (PM) emitted from combustion engines can be mitigated by using

* Corresponding author.
E-mail address: pravesh@iitbhilai.ac.in (P.C. Shukla).

https://doi.org/10.1016/j.clet.2024.100725
Received 24 September 2023; Received in revised form 24 December 2023; Accepted 12 January 2024
Available online 23 January 2024

specific injection parameters, fuel designs (alternative fuels and fuel additives) (Agarwal et al., 2013a; Sahu and Shukla, 2022a), advanced combustion technologies (Beatrice et al., 2017; Di Blasio et al., 2017, 2023), and aftertreatment systems (Joshi, 2023; Shukla et al., 2018). However, implementing these technologies adds capital costs to the engine in different applications, such as agriculture and construction. Combustion-generated suspended particles in the air are solid forms of pollutants that cause health hazards like asthma, respiratory diseases, carcinogenic problems, etc. (Shukla et al., 2017; Agarwal et al., 2013b). Particulates are composed of elemental carbon (EC), organic carbon (OC), and traces of sulphates, nitrates, and elements. Some organic components present in particulates are harmful, such as polycyclic aromatic hydrocarbons (PAHs) which are on the list of probably carcinogenic to humans (Group 2A) and possibly carcinogenic to humans (Group 2B) defined by the International Agency for Research on Cancer (IARC) (International Agency for Research on Cancer, 1989). In the above context, it is essential to understand the toxicity effects due to particulate emissions that contain these carcinogenic compounds. Wetstacking is another important issue in diesel engines, besides its harmful effect on humans and the environment, which causes engine failure; therefore, the measurement of PAHs becomes important (Yilmaz and Donaldson, 2005).

Alcohols are already used in SI engines in the form of blends with gasoline. They have been extensively studied, showing their potential to reduce CO_2 emissions (Awad et al., 2018; Di Luca et al., 2022). However, few studies are available for a higher fraction of alcohol utilization in CI engines (Sahu et al., 2022a). 30% ethanol fraction (*v/v*) in blend with diesel-biodiesel and diesel-gasoline (biodiesel and gasoline used as a solubilizer) in a light duty CI engine was investigated. Results proved significant improvement in efficiency and NOx-soot trade-off compared to diesel (Shamun et al., 2018; Belgiorno et al., 2018). Nour et al. (2019a) found that higher molecular weight alcohols, i.e., pentanol and octanol in diesel enhanced blending stability, engine performance and reduced emissions. They stated that higher alcohols (butanol, octanol, heptanol) in diesel reduce NOx and soot production at the expense of CO and HC (Nour et al., 2019b).

Thus, it can be drawn that alcohol blended with diesel usually reduces PM emissions (Shamun et al., 2018; Ianniello et al., 2021). On the other hand, the trend about morphological and toxicity characteristics of alcohol generated PM are not very obvious since they have not been investigated thoroughly. Maricq (2007) have explained the typical composition of diesel-generated PM, which consists of a branched agglomerated structure where the core is dry soot. This is normally covered with organic compounds, saturated, unsaturated, aromatic hydrocarbons, etc., with traces of metal elements and ash contents. Nord et al. (2004) reported chain-like agglomerations of particles in diesel emissions, while PM for ethanol engine was characterised by single and clumped particle agglomerations. The diesel particles formed by agglomeration were 600–800 nm in size. Ethanol particulate observed smaller sizes (~200 nm) (Nord et al., 2004). Chen et al. (2017) investigated the morphology of PM emitted for butanol diesel blends, they reported that the average diameter for the PM emitted from butanol blends is 0.85 μm and 0.52 μm for 5% and 10% butanol blends, respectively, which is 50% smaller compared to the diesel case. Ruiz et al. (2015) analysed the morphological characteristics of PM emitted from an ethanol/butanol-diesel fuel. They reported similar nanostructure and agglomerated particles for diesel and ethanol/butanol blends. It is reported that the morphology of PM samples for different ethanol-diesel ratios, and of E5, E10, and E15, reporting that the individual primary particles were in the range of 70–110 nm (Li et al., 2013). All the listed morphological studies provide the physical characteristics of PM generated from alcohol-diesel fuelled CI engines, but it is likewise important to perform chemical characterization and investigate the toxicity potential of the organic compounds associated with PM. PAHs with two rings exist almost exclusively in the gas phase at ambient temperature, while three or four rings may appear in gas as well as liquid phase. Moreover, PAHs with five or more rings are predominantly adsorbed on particles. Researchers have investigated the PAH emissions from engine out exhaust and its associated toxicity (Song et al., 2007; Paim et al., 2023; Merritt et al., 2005; Chang et al., 2013). Ethanol-diesel blends showed significant PAHs and benzene emission reductions in the order of ~19% and ~50%, respectively, with a substantial reduction in nitro based toxic compounds. In particular, exhaust associated PAHs investigations performed by Paim et al. (2023) and Chang et al. (2013) showed reductions of 40% and 31% in total PAHs for ethanol and acetone-butanol-ethanol blends with diesel, respectively. Yilmaz et al. (2022)and Yilmaz and Davis (2016) found ~70% reduction in PAH toxicity level for alcohol (20% *v/v*) in biodiesel blends albeit an increased toxicity level of about ~35%, and mainly due to higher benzo [a]pyrene fraction. Butanol in diesel showed ~75% reduction (for 10% butanol blend) and 5-fold increase (for 50% butanol blend) in the toxicity level of PAHs compared to diesel (Yilmaz and Davis, 2022a, 2022b). Moreover, 1% *v/v* water emulsion drastically increased the toxicity level, and it also increases the risk of wetstacking in CI engines (Yilmaz and Davis, 2022a). While Malmborg et al. (2017) have observed that the accumulation behaviours of PAHs have increased using exhaust gas recirculation (EGR).

The chemical characterization of biodiesel-generated PM revealed the presence of PAHs and trace metals, and the mutagenic and cytotoxic potential was higher than their diesel counterparts (Agarwal et al., 2018), demonstrating that the aftertreatment devices may be effective in reducing their concentration. This is also confirmed by Hu et al., 2013 which observed a 90% reduction in PAHs emissions by using aftertreatment systems (ATS) in a heavy-duty engine.

Karavalakis et al., 2011 investigated the impact of different biodiesel blends on unregulated emissions from a passenger car, including PAHs, demonstrating that biodiesel blends resulted in higher PAHs compounds. This was due to the presence of cyclic acids and polymerization products and the degree of unsaturation in the biodiesel blends. Another study performed by the same research group (Karavalakis et al., 2010) reported that using biodiesel resulted in notable increases in low molecular-weight PAHs such as phenanthrene and anthracene. They also found that biodiesel led to a decrease in *nitro*-PAHs and large PAHs, which are known for their mutagenic and carcinogenic properties. The hydrogenated vegetable oil (HVO) and HVO-biodiesel blends have shown reduced low-molecular-weight PAHs emissions in a typical CI engine (McCaffery et al., 2022). Agarwal et al., 2020 noted that the gasohol-powered SI engine emitted lower concentrations of unregulated gaseous species, fewer particles, and lower concentrations of hazardous PAHs and trace metals.

Based on the current literature review, there is no evidence of the investigation of PM morphology and PAHs formation from alcohol-diesel blends in a ratio 50:50 in high compression ratio (26:1) CI engines. PAHs characterization of higher fraction of alcohol fuelled CI engines have been investigated by other studies with conventional CR only by modifying the operating parameters such as pre-heating the air, dual fuel injection strategy, etc. This study attempts to investigate the PM morphology and associated PAHs toxicity of higher fractions of methanol (up to 20% *v/v*), ethanol and butanol (up to 50% *v/v*) in diesel and fuelling a high compression ratio (CR26) CI engine. The novelty consists mainly in the PM morphological characterization, speciation of PAHs, and the evaluation of PAHs associated toxicity equivalent factor emanating from a high compression ratio CI engine. In particular, a toxicity equivalent factor evaluation for individual PAHs (potential occupational carcinogenic as per NIOSH) generated from a high CR compression ignition engine fuelled with methanol-diesel, ethanol-diesel, and butanol-diesel blends is carried out providing new insights in comparison to what already available in the scientific literature. Several PAHs, including low molecular weight (LMW) PAHs, high molecular weight (HMW) PAHs, and *nitro*-PAHs, are investigated for methanol-diesel, ethanol-diesel, and butanol-diesel blends. High fractions of alcohol (up to 50% *v/v* in diesel) in blends were tested, defining new

Table 1
Test engine specifications.

Engine model	Kirloskar DM10
Engine type	4-stroke CI engine coupled with generator
Number of cylinders	1
Bore	102 mm
Stroke	116 mm
Displacement	948 cm^3
Compression ratio	17.5:1 (diesel) and 26.0:1 (alcohol-diesel blends)
Maximum power output	7.4 kW at 1500 rpm

limits to their applications in a typical CI engine widely used for power generation applications.

2. Experimental setup and methodology

This work presents a detailed morphological study of PM emission, PAHs speciation, and toxicity assessment for the particulates collected from a high compression ratio CI engine fuelled with alcohol fuel blends. A single-cylinder, 0.948 *l*, water-cooled, conventional power generator diesel engine was used for this purpose, which is commonly available and used in India for many rural and sub-urban agricultural and power generation applications. The engine was equipped with temperature and pressure sensors at the salient points, and the piston bowl was properly modified to increase the CR from 17.5:1 to 26:1 to facilitate the auto-ignition for a higher fraction (up to 50% *v/v*) of alcohol-diesel blends. The engine specifications are reported in Table 1.

Fig. 1 shows the experimental setup and the partial flow dilution tunnel used for the PM sampling. The partial flow dilution tunnel samples a fraction of exhaust flow from the engine exhaust manifold iso-kinetically, which can then be diluted with fresh treated and filtered air in a desired proportion (dilution ratio). For this study, the air-to-exhaust dilution ratio was kept constant at 16:1 during the sampling. The dilution ratio was calculated by the following formula (eq. (1)):

$$Dilution\ ratio\ [\%] = \frac{CO_{2\ exhaust}}{(CO_{2\ diluted} - CO_{2\ air})} \times 100 \quad (1)$$

Quartz filter substrates (φ 47 mm) were used for PM sampling of different fuels using a filter holder assembly fixed at the end of the partial flow dilution tunnel. Filter papers were conditioned in a desiccator for 24 h to remove the unwanted moisture content before the sampling. PM sampled on quartz substrates were measured for diesel at a conventional compression ratio (CR17.5), and alcohol blends at a higher compression ratio (CR26). These PM samples were analysed for morphological characterization using a field emission scanning electron microscope (FESEM) (at 25,000X and 100,000X magnification). Carl Zeiss microscopy (Model: Gemini SEM 500) was used to examine the microstructure of PM. FE-SEM is based on the principle of using a focused, high-energy electron beam to scan the surface of a sample and generate signals that provide information about its morphology, and composition. Since the PM samples are non-conductive, gold sputtering was performed for each sample. Smoke opacity was also measured during the experiments using the smoke analyzer (AVL-MDS450). PM sampling has been performed for a relatively long duration under steady-state conditions of the engine operation. Each test sampling for PM collection was performed for 15 min only after the engine stabilized thermally. The collected samples on quartz filter paper were analysed to identify specific PAHs present in the PM sample collected using liquid chromatography with high-resolution mass spectrometer (LCMS). LCMS (Make: Agilent; Model: 6545XT AdvanceBio LC/Q-TOF), located at the Central Instrumentation Facility of IIT Bhilai, was used to identify, quantify, and speciate PAHs. A quarter part of the collected PM of know mass was taken for the sample preparation for PAHs analysis in LCMS. This was then dissolved in 2 ml of ultra-pure methanol using a 5 ml vial, followed by ultra-sound sonication for 30 min. The solution was centrifuged at 10,000 rpm for 15 min to separate any possible solid content present in the solution. The centrifuged solution was filtered using 0.2 μm filter media, and a small volume of 50 μl prepared sample was adjusted to 1 ml using ultra-pure methanol. The prepared samples were introduced into the LCMS system for analysis. The chromatograms obtained from LCMS were examined to analyse the presence of PAHs, *nitro*-PAHs, and other organic fractions in the tested sample.

LCMS has an accuracy level of 2 ppm for the PAHs measurement. It may be noted that the PAHs measurement is complicated, and its uncertainty may vary in a significantly large range of measurement values. The present analysis attempted to compare the PAHs emanating using methanol, ethanol, and butanol blends with diesel.

The present study is mainly focused on investigating low molecular weight alcohols; therefore, methanol, ethanol, and butanol blends were used at different proportions with diesel. A part-load operating condition was chosen, with an engine speed of 1200 rpm and 2.0 kW of generator power output to compare PM emissions and assess the toxicity of particulate PAHs in diesel and alcohol-diesel blends. The tested engine load condition was used because literature shows higher PAHs emission at lower load conditions while it starts reducing with increasing engine load (Yilmaz and Davis, 2022a; Yusuf et al., 2022).

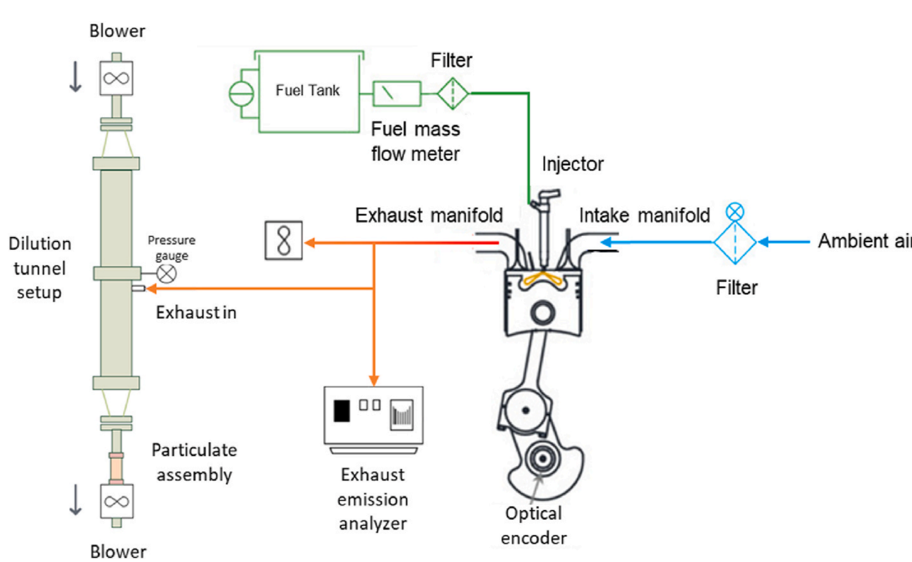

Fig. 1. Experimental engine test setup.

Table 2
Test fuel properties (Verhelst et al., 2019; Sahu and Shukla, 2022b; Alemahdi and Tuner, 2020; Zhang et al., 2011, 2023).

Property parameters	Diesel	Methanol	Ethanol	Butanol	M20	E20	E50	B20	B50
Density at 15 °C, kg/m^3	832.7	790	785	810	823.6	822.6	808.5	827.6	821
Kinematic viscosity at 40 °C, mm^2/s[a]	2.13	0.59	1.2	2.51	1.64	1.89	1.59	2.20	2.31
Calorific Value, MJ/kg	43.0	20.2	27.1	33.1	38.4	39.8	35.1	41.0	38.1
Autoignition temperature, °C	250	363	385	343	–	–	–	–	–
Latent heat of vaporization, kJ/kg	270	1178	838	585	451.6	383.6	554	333	427.5
Flashpoint, °C	57	12	12	37	–	–	–	–	–
Oxygen, max wt%	0	50	34.8	21.6	9.6	6.9	17.4	4.3	10.8
Carbon, max wt%	86.1	37.5	52.2	64.8	76.3	79.3	69.1	81.8	75.4
Hydrogen, wt%	12.9	12.5	13.0	13.6	12.8	12.9	12.9	13.0	13.2
Carbon-to-hydrogen ratio (C/H)	6.5	3.0	4.0	4.7	5.9	6.1	5.3	6.2	5.6
Stoichiometric air-fuel ratio, kg/kg	14.5	6.6	9.0	11.1	12.9	13.4	11.75	13.8	12.8
Cetane number	51.4	4	8	25	–	–	–	–	–

[a] Fuel blend values for kinematic viscosity are evaluated using the method given by Zhang et al., 2023).

This happens because lower overall average combustion temperatures result in incomplete combustion of fuel and lube oil hydrocarbons and lead to the formation of pyrolyze compounds, which eventually are the building blocks for multi-ring structured PAHs.

Five different alcohol-diesel blends (*v/v*), in particular, 20% methanol in diesel, 20% and 50% ethanol in diesel, and 20% and 50% butanol in diesel. Before the sampling started, the engine was allowed to reach the steady state condition during the experiment. All the sampling and measurement equipment were calibrated properly before the PM sampling and analysis to minimize errors in the results.

Table 2 shows the main physico-chemical properties of diesel, methanol, ethanol, and butanol. This table also indicates the calculated blended fuel properties from the base fuel properties i.e., for M20, E20, E50, B20 and B50. It can be noted that the density, viscosity, and calorific value of alcohol fuels are significantly lower compared to diesel. Alcohol possesses higher latent heat of evaporation and auto-ignition temperature than diesel. These results in longer ignition delay and a higher rate of heat release, thus affecting the combustion and emission characteristics compared to the conventional diesel, limiting the higher volume fraction utilization of alcohols in a CI engine. Methanol, ethanol, and butanol (Table 2) show 21.6%, 34.8%, and 50.0% of oxygen content (*m/m*), carbon to hydrogen (C/H) ratio is up to 50% lower for alcohols, and the stoichiometric air-fuel ratio is also lower in comparison to diesel.

Alcohol fuel generally shows a phase separation phenomenon when blended with diesel in the presence of atmospheric air. This happens because of the absorption of atmospheric moisture in alcohol molecules in the form of hydrates. Moisture absorption leads to the phase separation of alcohol and diesel in the blend which causes trouble in the fuel injection system and results in poor combustion process. Thus, it is important to evaluate the stability of the alcohol-diesel blend by modifying the fuel design. Studies (Shanmugam et al., 2021; Lei et al., 2012; Singh and Bharj, 2019) show that certain additives can be doped in the fuel blend to avoid the separation phenomenon for a relatively (a few days) longer time duration. Shanmugam et al., 2021 reported that 1% oleic acid doping in alcohol blends (tested for E30) provided fuel stability. In the present study, authors have doped 1% of oleic acid with alcohol blends, and the fuel blend stability characteristic evaluation was performed before the engine experimental activities. All the blends for the engine experiments were prepared to avoid any phase separation during the testing. Each test was performed within 90 min from the respective blend preparation and no separation phenomenon was observed.

3. Results and discussion

This section discusses the experimental results obtained from alcohol-diesel blends (methanol, ethanol, and butanol) fuelled high compression ratio (CR26) CI engine focusing on the morphological characterization of PM and toxicity potential of PAHs.

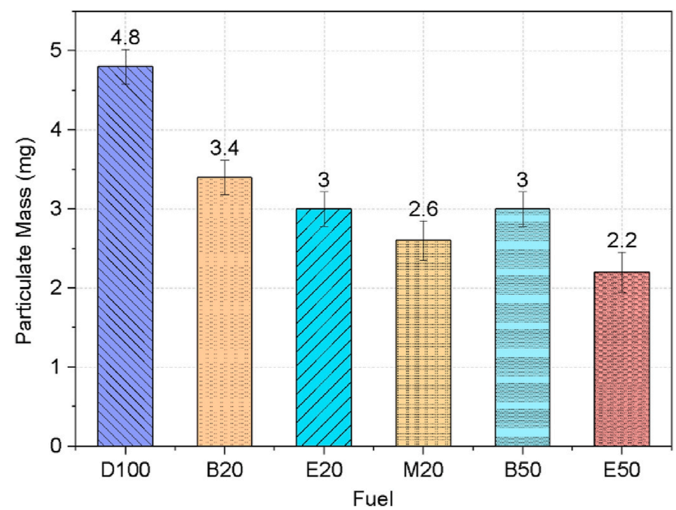

Fig. 2. PM emission for diesel (CR17.5) and alcohol-diesel blends (CR26).

3.1. PM emissions

In this section, PM and smoke opacity have been discussed for the tested alcohol-diesel blends (at CR26) and compared to conventional diesel combustion (at CR17.5). Experiments were performed at 1200 rpm and 2 kW of generator output, which is a moderate load condition for this specific engine. PM samplings (for each tested fuel) were performed for 15 min on 47 mm quartz filter papers using a partial flow dilution tunnel, which was sufficient duration to collect a reasonable mass of PM for PAHs analysis. It has been observed that PM emissions were reduced for the 20% alcohol blends (*v/v*) (Fig. 2) in comparison to diesel, and M20 resulted in the lowest amount of PM. It should be noted that methanol usually shows superior atomization characteristics compared to ethanol and butanol, which is in line with the spray characterization studies (Badawy et al., 2022, Azami and Savill, 2016).

Moving towards the higher blending of alcohols (B50 and E50), the further reductions of PM emissions were not in the relative proportion of alcohol fractions. For example, E20 and B20 significantly reduced the PM emission (~37% and ~29%, respectively) compared to conventional diesel combustion, while E50 and B50 showed ~54% and ~38% reductions. These results are similar to the findings obtained by Xiao et al., 2020, which performed tests with increasing butanol fraction in biodiesel (0–30%). The formation of gas phase hydrocarbons (leads to soluble organic fraction formation) and reduction in dry soot combinedly reduces the overall effect of PM reduction (Chen et al., 2007) for a higher fraction of alcohol in diesel.

Fig. 3 indicates the smoke opacity measurements showing similar trends as it is for PM mass emission (except E50). Particulate formation

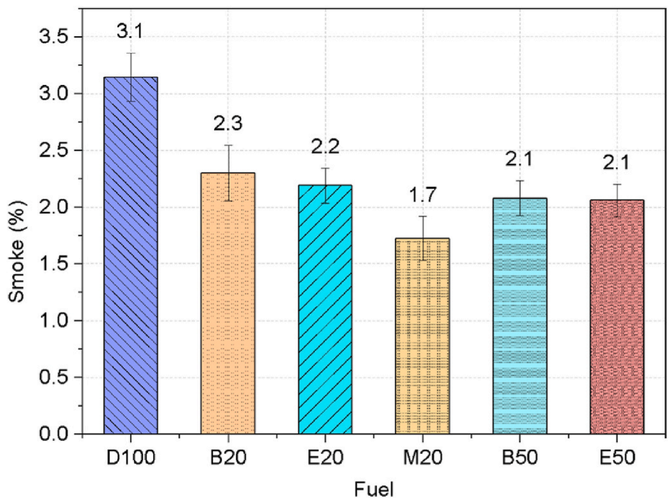

Fig. 3. Smoke opacity for diesel (CR17.5) and alcohol-diesel blends (CR26).

derives from the pyrolysis process during the combustion. In the case of diesel, long-chain hydrocarbons break and eventually lead to the formation of smaller lengths of hydrocarbons. Also, hydrogen escapes the molecule under high pressure and temperature of combustion which results in pyrolysis (higher C/H ratio), leading to soot formation. The presence of alcohol in the blend causes a lower degree of pyrolysis during the combustion which results in lower PM (Song et al., 2007; Shukla et al., 2014; Kim et al., 2002; Rana et al., 2022).

3.2. Soot morphological analysis

Particulate matter emitted from diesel engines is complex in its constituents and its physical structure. Microscopic analysis of diesel particulates in earlier studies shows complicated branched dendritic structures. In this study, detailed morphological observations of PM collected for diesel and alcohol blends (B20, E20, M20, B50, and E50) for high compression ratio CI engine showed significantly higher PM (Fig. 4) for diesel in comparison to alcohol-diesel blends when engine operating at 1200 rpm and 2 kW load. SEM images show that the particulates, emitted from diesel combustion partially cover the fibres of the substrates, and fluffy bulk lumps of carbonaceous materials can be observed. The morphology of diesel particulates indicates a branched and sticky nature, as seen in Fig. 4a. It exhibits a higher degree of agglomeration behaviour (visible in the form of growing dendrites) during the particle formation process from the morphology of the collected particulates of diesel combustion. The PM flocs are formed by the agglomeration of nucleation mode particles where the core consists

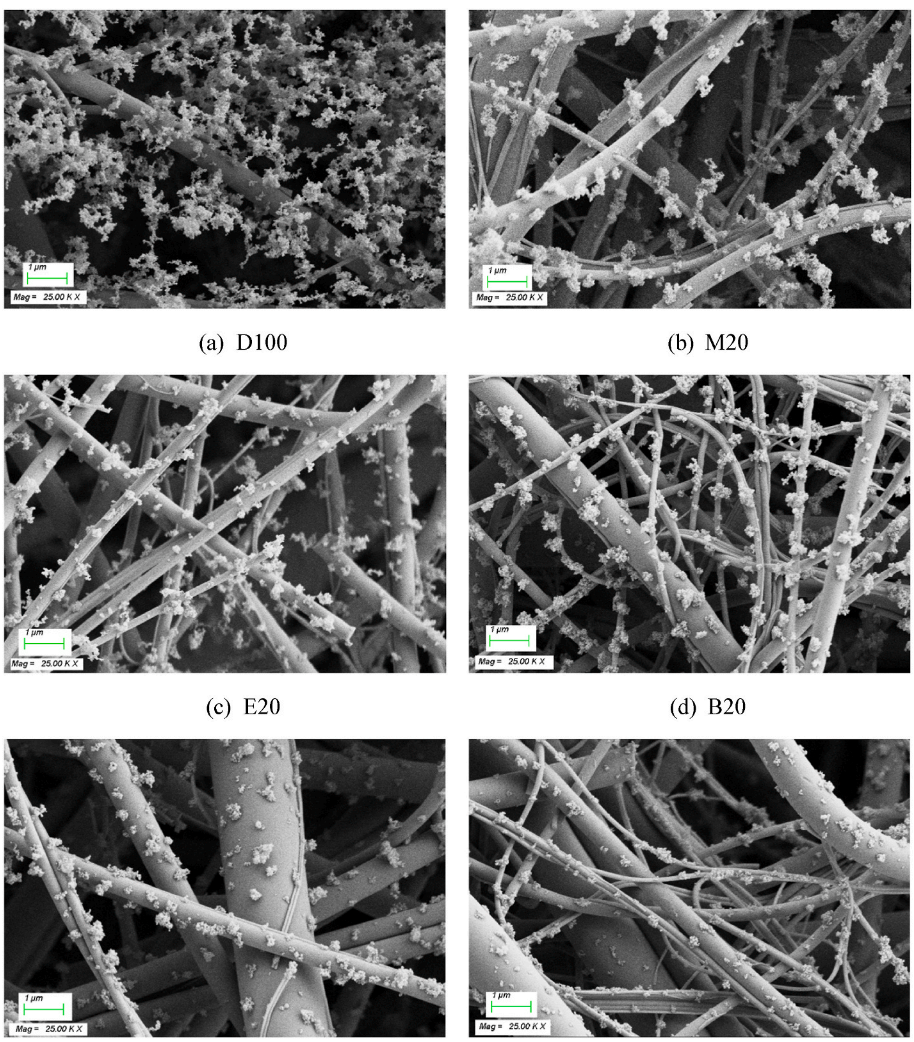

(a) D100 (b) M20

(c) E20 (d) B20

(e) E50 (f) B50

Fig. 4. SEM images of particulate samples for diesel (CR17.5) and alcohol-diesel blends (CR26).

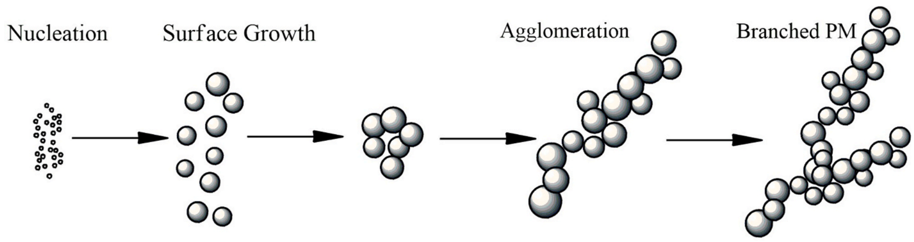

Fig. 5. Particle formation and surface growth, redrawn and conceptualized from (Eastwood, 2008).

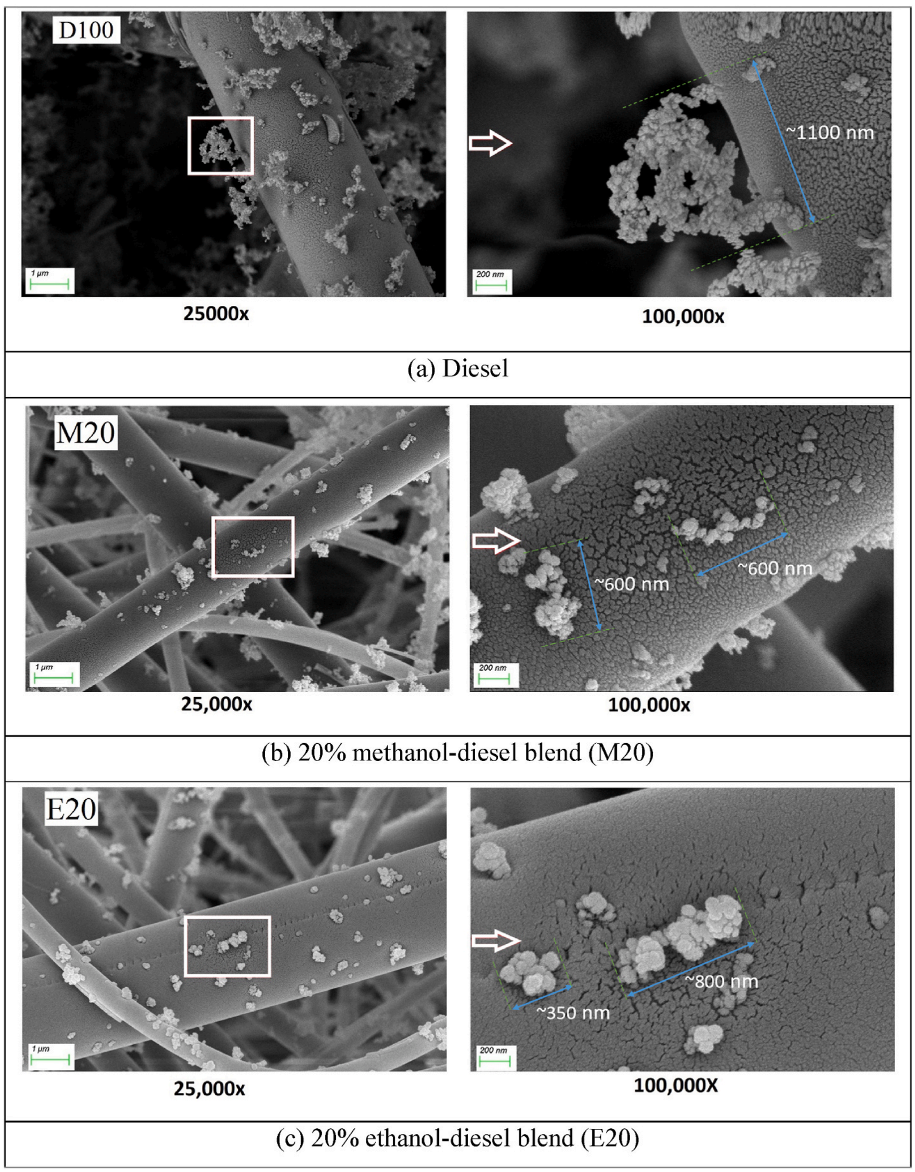

Fig. 6. Morphological characteristics for diesel (CR17.5) and alcohol-diesel blends (CR26) particles.

of carbonaceous material, which is normally covered by organic carbons (Maricq, 2007). These branched agglomerated particles provide high surface areas that come up with sites for the adsorption/absorption of various organic compounds generated during combustion and post-combustion (Xu et al., 2021). A representation is shown for the agglomeration process and the typical branched particulate structure in Fig. 5.

Fig. 4b, c, and 4d show the PM emissions for M20, E20, and B20, respectively, under high compression ratio operating conditions. The figures show the discrete individual lumps with a much lower degree of particle agglomeration behaviour than the conventional diesel combustion particulates. Thus, it can be stated that these particles provide a much lower area for the adsorption/absorption of the organic compounds. This means alcohol particles have the potential to discourage the adsorption/absorption of harmful organic compounds. These tiny fine particles can easily be inhaled deeper into our respiratory system

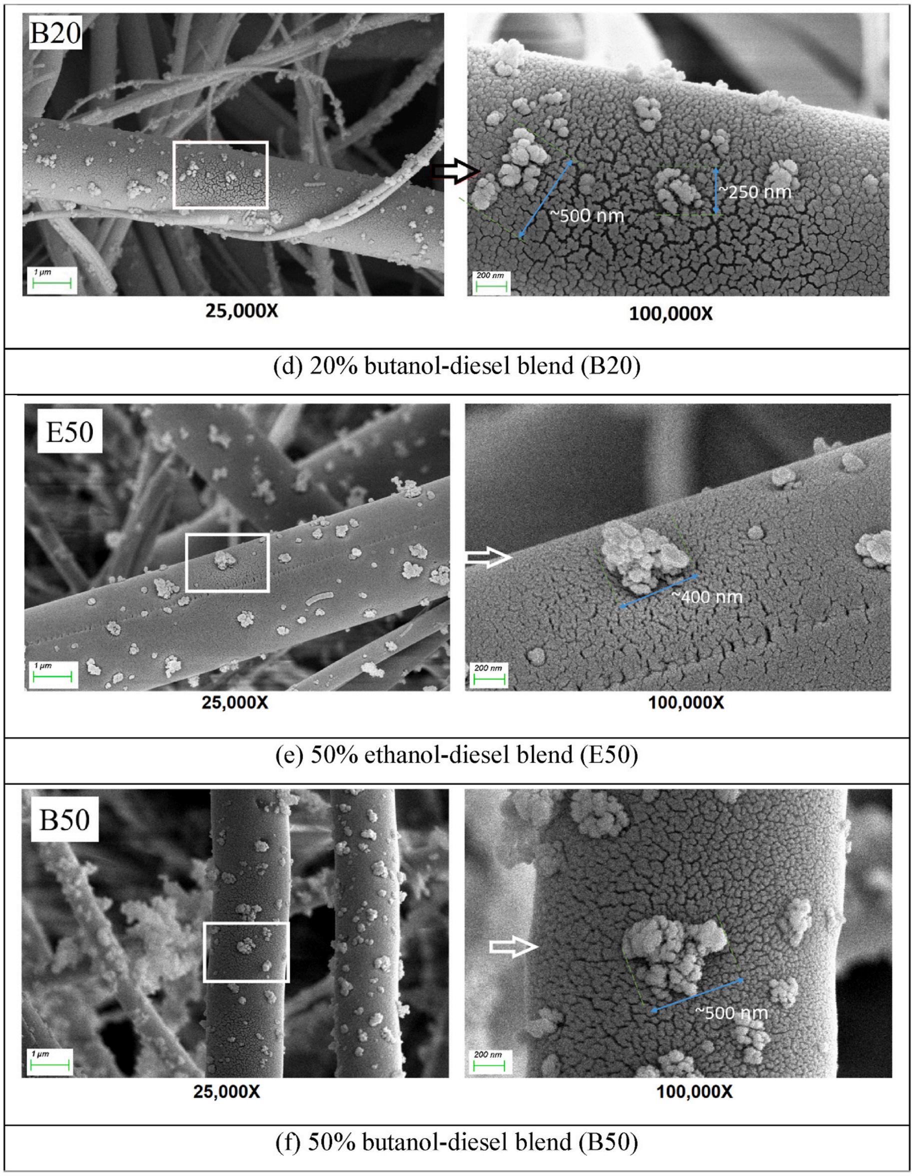

Fig. 6. (*continued*).

and further can enter the bloodstream (Kittelson, 1998; Medina et al., 2007; Pierdominici et al., 2014; Otsuki et al., 2014). Looking at Fig. 4, diesel resulted in denser and larger-sized particles compared to 20% of alcohol blends. The particle collection density on the substrate is reduced (Fig. 4) when the blending fraction of ethanol and butanol increases up to 50% (*v*/*v*).

Fig. 6 uses SEM to show the morphology of single agglomerated particles of the tested fuels at 25,000X and 100,000X magnifications. The magnified image of diesel particulates, in Fig. 6a highlights that the quartz fibres act as sites for the collection of branched agglomerated particles under the effect of various deep filtration methods such as inertial impaction, adsorption, deposition/re-entrainment, sedimentation, and turbulent deposition, etc. Fig. 6b, c, and 6d show the morphology of the particulates collected for M20, E20, and B20, respectively. These images show a common characteristic of the relatively small size of particles with lower collection density in comparison to the diesel particles (Fig. 6a). Particulates are collected for diesel and alcohol blends (100,000X images; Fig. 6). Diesel particulates show that the smaller nucleation mode particles agglomerate and form a larger branched type of agglomerated particles (white box in Fig. 6a). This formation is absent in the case of M20, E20, and B20 generated particles (Fig. 6b, c, 6d). Diesel fuel is mainly composed of long chain hydrocarbon, which stimulates the pyrolysis process during combustion. This leads to higher PM emissions with larger sizes of branched agglomerated structures. Also, significant organics are presented in diesel particles emanating from partial/incomplete combustion of lubricating oil and fuels (Agarwal et al., 2011; Wang et al., 2016). In the case of alcohols, the carbon chain length is relatively smaller than diesel fuel, and it also contains oxygen inherently (Yesilyurt et al., 2020). These factors help in a higher degree of complete combustion and lower pyrolysis process. Lower PM emission and a lower degree of pyrolysis in the case of alcohols might result in a relatively small size and lower overall mass of particles. A similar result has been reported by Kalwar et al., 2020). Fig. 6 also compares the particulates generated from the alcohol blends used. The PM for methanol shown in Fig. 6b consists of a limited number of nucleation mode particles and forming agglomerated particles. Concerning the size ranges, agglomerated particles for diesel can be observed, and particulate size up to 2000 nm; however, for alcohol-diesel blends, it is in the range of 400–600 nm (Fig. 6). One of the possible reasons is to have lower organic in the case of alcohol blends, and therefore the size of agglomerated particles is relatively smaller compared to diesel particulates. The presence of organics may

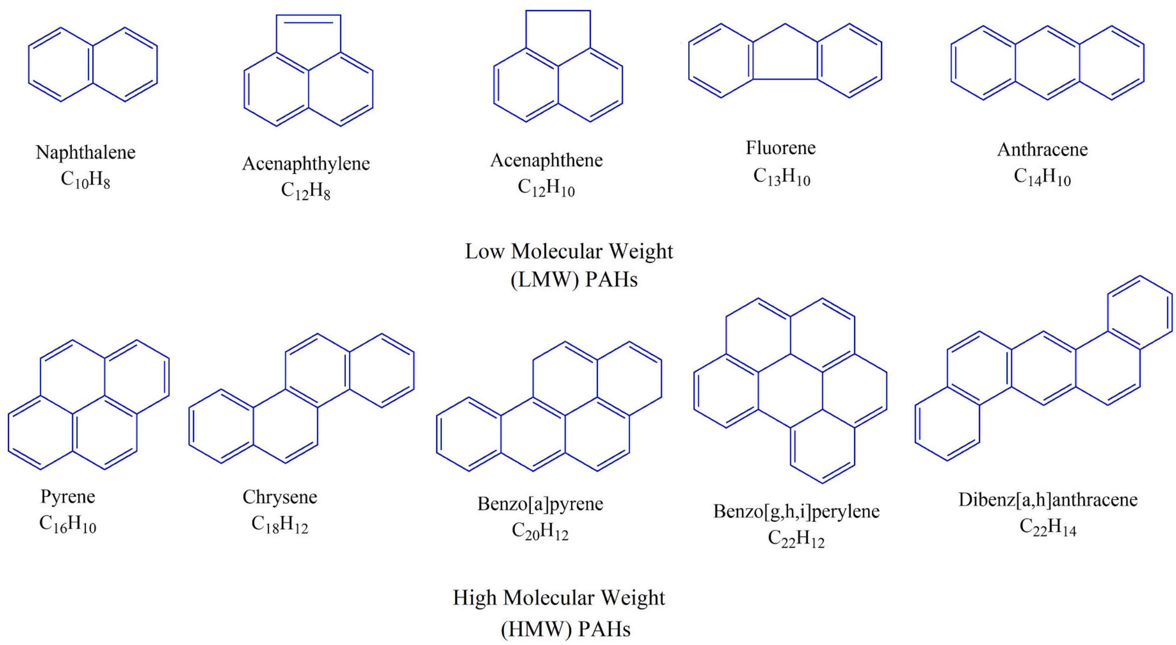

Fig. 7. Chemical structure of PAHs compounds, redrawn from (Ravindra et al., 2008).

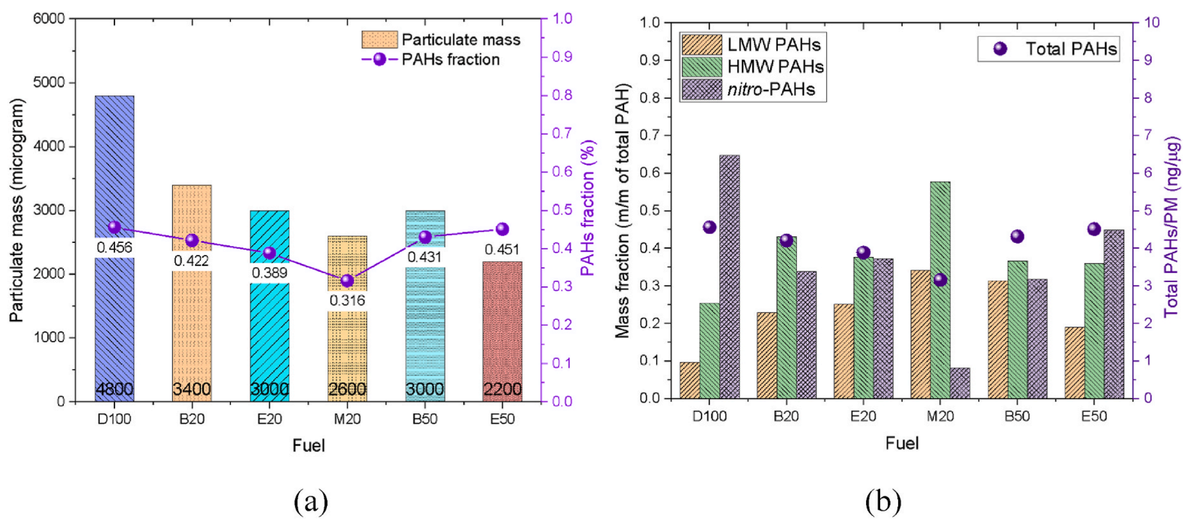

Fig. 8. Total PAHs/PM, mass fraction of LMV, HMV, and *nitro*-PAHs for diesel (CR17.5) and alcohol-diesel blends (CR26).

help in a higher degree of agglomeration (togetherness behaviour of different nucleation mode particles), and therefore, diesel particulates might result in a large size range compared to alcohol blended particles. E50 and B50 generated PM indicated similar morphological characteristics to that of E20 and B20 as observed in Fig. 6.

3.3. Polycyclic aromatic hydrocarbons (PAHs) emissions

Section 3.2 of this study mostly includes the qualitative characterization of PM mass emissions using mass measurement and microscope imaging, respectively. Numerous studies (Nisbet and Lagoy, 1992; Ravindra et al., 2008; Rajeev et al., 2023) have shown that polycyclic aromatic hydrocarbons (PAHs) are one of the major constituents in PM mass emissions from a toxicity point of view. The present section reports the PAHs emissions and their implication on the overall toxicity potential. PAHs are produced as a result of the pyrolysis process during the combustion of fuels. Under high temperature and pressure conditions, straight-chain hydrocarbons result in the formation of cyclic aromatic compounds (hydrogen stripped-off partially) comprising two or more benzene-like rings due to the lack of locally available oxygen. PAHs have been classified into three categories named as low molecular weight PAHs (LMW), high molecular weight PAHs (HMW), and *nitro*-compounds of PAHs (Fig. 7) (Rajeev et al., 2023).

PM in the exhaust may contain several different PAHs, however, the study reported ten important PAHs, namely: naphthalene, acenaphthylene, acenaphthene, fluorene, anthracene, pyrene, chrysene, benzo[a]pyrene, dibenzo[a,h]anthracene and benzo[g,h,i]perylene, categorized under LMW, HMW and *nitro*-PAH. LMW PAHs contain PAHs with two or three benzene rings, and HMW PAHs contain higher PAHs with four or five benzene rings, also considered to be more toxic and carcinogenic compared to LMW PAHs (Rajeev et al., 2023). Fig. 8 shows the total fraction of PAHs (LMW + HMW + *nitro*-PAH) out of the total particulate mass collected on filter paper, it is in the range of 0.3%–0.5% of the total PM weight. Diesel shows 0.5% PAHs of total PM mass, and the lowest PAHs fraction was observed for M20 fuel. Total PAHs fraction is in a downtrend from higher carbon alcohol to lower carbon alcohol.

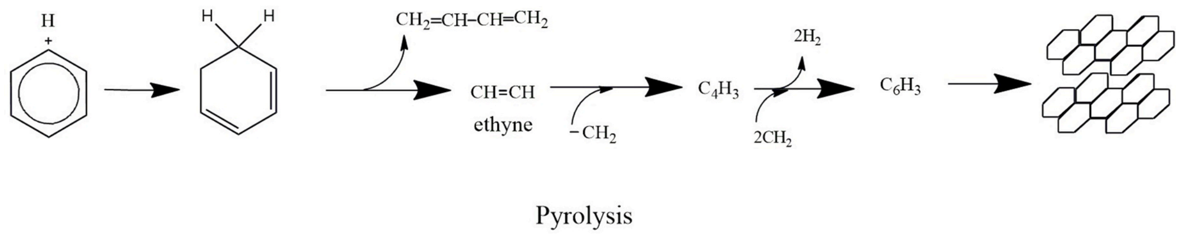

Fig. 9. PAHs formation mechanics, redrawn and conceptualized from (Van Setten et al., 2001).

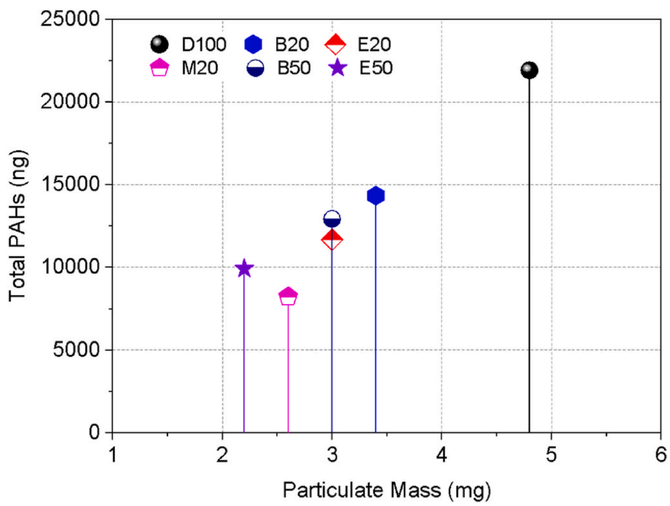

Fig. 10. Total PAHs function of particulate mass for diesel (CR17.5) and alcohol-diesel blends (CR26).

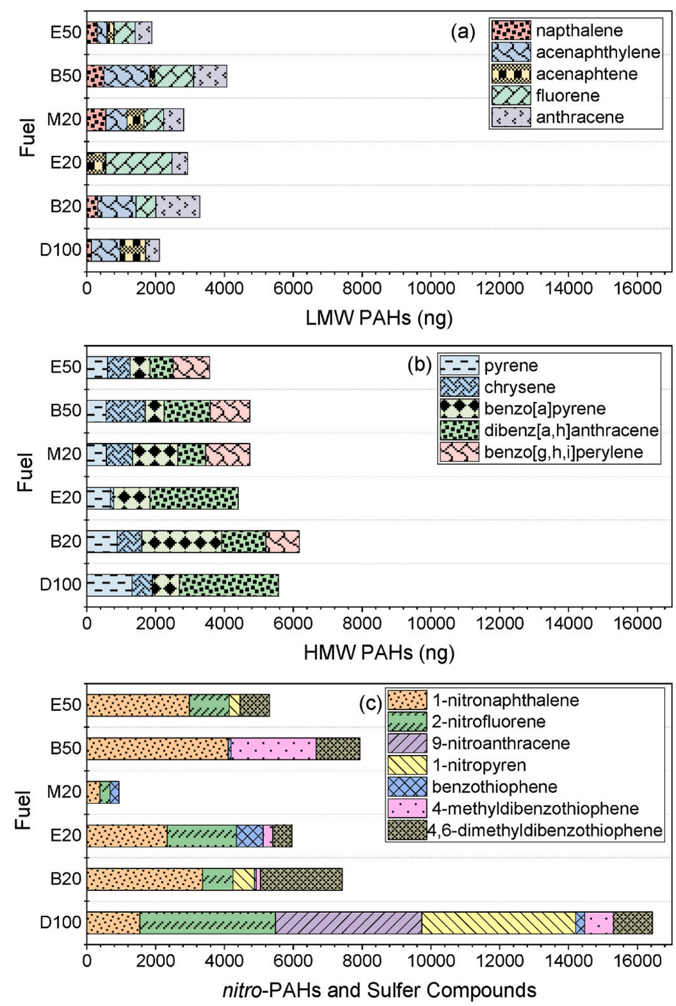

Fig. 11. Mass concentrations of LMW, HMW, and *nitro*-PAHs for diesel (CR17.5) and alcohol-diesel blends (CR26).

One of the possible reasons for lower PAHs emission in the case of alcohol blends is the lower carbon chain, which reduces the pyrolysis process, resulting in lower PAHs formation during fuel combustion.

Fig. 8 shows the mass fraction of PAHs for the tested fuels. The total PAHs emission for diesel contributes the highest fraction of *nitro*-PAHs (reaching up to 65%). IARC report (International Agency for Research on Cancer, 1989) suggests that *nitro*-PAHs possess a significantly high degree of toxicity potential. The alcohol blends resulted in a reduced fraction of *nitro*-PAHs compared to diesel (Paim et al., 2023). This reduced fraction of *nitro*-PAHs is compensated by LMW and HMW for alcohol blends. Zhao et al., 2022 and Tse et al., 2015 observed that alcohol blends with diesel have shorter combustion duration. Thus, conversion of *nitro*-PAHs from PAHs through electrophilic nitration (Ghadikolaei, 2016) (addition of NO_2 in benzene ring) reduces, lowering the overall *nitro*-PAHs formation in PM of alcohol blends. Fig. 9 indicates the mechanism of PAHs formation during combustion (Van Setten et al., 2001). Diesel contains long straight chain hydrocarbons, which result in C_2H_2 precursors during the combustion process which serve as raw materials for the formation of single ring benzene like compounds and multiple rings PAHs (Fig. 9).

Total PAHs per unit mass of PM were reduced with the use of alcohol fuels, however, tested fuels (ethanol, methanol, and butanol blends) resulted in varying concentrations of any specific PAHs, which is mainly due to different behaviour of fuel during combustion and pyrolysis process. Among the tested alcohols, M20 indicated the lowest fraction of *nitro*-PAHs, however, the fraction of HMW in total PAHs increased significantly. Xu et al., 2022 investigated that M20 resulted in a higher chemical reaction rate with higher laminar flame speed. This reduces the combustion duration and thus conversion of PAHs to *nitro*-PAHs (it involves OH radical attack and subsequent addition of $–NO_2$) (Ghadikolaei, 2016), resulting in lower *nitro*-PAHs for M20. It can be noted that the increment in the blend ratio of ethanol and butanol does not make any significant difference in the PAHs fraction in total PM emissions. These two blends are also consistent in *nitro*-PAHs emission for the tested blend ratio. Similar to the lower PM shown in Figs. 2 and 8 also exhibits the lowest total PAHs emission for M20.

Looking at the PAHs/PM (ng/μg) index, diesel, and E50 show similar results, 4.31 ng/μg, and 4.51 ng/μg, respectively. However, the absolute PAHs emission is reduced by a factor of two in the case of E50 since the PM emissions are almost half. Fig. 10 shows the relation between total PM and total PAHs for different fuels, higher for diesel and significantly lower for alcohol blends. The individual concentration of PAHs (Fig. 11) looks completely different, which affects the overall toxicity potential of the fuel. Toxicity assessments were performed for all the fuels, which is discussed in later section 3.4 to evaluate the toxicity of the PM sample for all tested fuels.

Table 3
Toxicity equivalent factor (TEF) and toxicity potential (TP) of PAHs for tested fuels (Agarwal et al., 2013b; Nisbet and Lagoy, 1992).

Chemical Name	Formula	Toxicity Equivalent Factor (TEF)	Toxicity Equivalence (TP) of Fuel (ng of Benzo[a]pyrene)					
			D100	B20	E20	M20	B50	E50
Naphthalene	$C_{10}H_8$	0.001	0.136	0.314	0	0.555	0.503	0.302
Acenaphthylene	$C_{12}H_8$	0.001	0.832	1.119	0	0.616	1.335	0.285
Acenaphthene	$C_{12}H_{10}$	0.001	0.741	0	0.555	0.487	0.138	0.204
Fluorene	$C_{13}H_{10}$	0.001	0	0.575	1.930	0.577	1.127	0.614
Anthracene	$C_{14}H_{10}$	0.010	4	12.82	4.51	5.79	9.67	4.82
Pyrene	$C_{16}H_{10}$	0.001	1.310	0.881	0.683	0.565	0.559	0.599
Chrysene	$C_{18}H_{12}$	0.010	5.97	7.13	0.99	7.63	11.38	6.63
Benzo[a]pyrene	$C_{20}H_{12}$	1.000	779	2326	1055	1311	550	574
dibenzo[a,h] anthracene	$C_{22}H_{14}$	1.100	3183.4	1412.4	4259.2	898.7	1480.6	739.2
Benzo[g,h,i]perylene	$C_{22}H_{12}$	0.010	0	9.72	0	12.90	11.51	10.67
1-nitronaphthalene	$C_{10}H_7NO_2$	0.100	154.3	335.8	234.1	38.7	411.3	298.3
2-Nitrofluorene	$C_{13}H_9NO_2$	0.100	393.8	88.8	200.7	27.9	0.0	115.0
9-nitroanthracene	$C_{14}H_9NO_2$	0.100	425.3	0.0	0.0	0.0	0.0	0.0
1-nitropyren	$C_{16}H_9NO_2$	0.100	446.9	62.1	0.0	0.0	0.0	32.1
Total			5395.8	4257.7	4319.7	2305.5	2478.2	1782.8

Fig. 11 categorizes the PAHs according to the molecular weight as previously defined, i.e., a) LMW, b) HMW, and c) *nitro*-PAHs. It has been observed that *nitro*-PAHs contribution is highest, in general, except for M20. M20 exhibits the minimum total PAHs and *nitro*-PAHs in comparison with the other tested fuels. The higher flame speed of methanol combustion (Xu et al., 2022) and shorter combustion duration persist for the lower concentration of *nitro*-PAHs formation (Ghadikolaei, 2016), allowing relatively lower time for conversion of PAHs to *nitro*-PAHs, i.e., OH radical joins and subsequent addition of NO_2.

Although M20 resulted in the lowest *nitro*-PAHs concentration, the total PAHs concentrations can be seen (Fig. 11) in a similar range obtained for the other test fuels due to the relative increase of HMW PAHs. Test performed with diesel resulted in the highest concentration of *nitro*-PAHs compared to the alcohol blends. However, LMW and HMW PAHs concentrations for diesel are comparable to the tested fuels. Looking at the HMW, the PAHs concentration can be observed in the range of 4000–6000 ng. E20 and diesel have shown significantly higher concentrations of dibenzo[a,h]anthracene in the total HMW (Fig. 11b). It should be noted that the toxicity equivalent factor of dibenzo[a,h] anthracene is 1.1 which is approximately 10 to100 fold higher compared to the other major HMW-PAHs emitted during the tests. M20 and B20 interestingly resulted in higher concentrations of benzo[g,h,i]perylene, which are ~1311 ng and ~2326 ng, respectively (Fig. 11), compared to the other fuels. For a higher blend of butanol (B50), 1-nitronaphthalene and 4-methyldibenothiophene concentrations were obtained significantly higher which indicates that B50 tends to promote the *nitro*-PAHs fraction. It can be concluded that diesel fuel shows higher *nitro*-PAHs out of total PAHs, moreover, the distribution of PAHs changes and shifts toward LMW and HMW PAHs, with a reduction in *nitro*-PAHs with the use of alcohol fuels. The above results (Fig. 10) highlight that the total PAHs emissions were significantly lowered using alternative fuels under the high compression ratio CI engine tests.

3.4. Toxicity assessment for PAHs

PAHs are complex combinations of different low and high molecular cyclic compounds (two or more benzene building blocks) with varying toxic potential. It is important to evaluate the toxic potential of different PAHs with the same reference and therefore, several researchers (Agarwal et al., 2013b; Yilmaz et al., 2022; Nisbet and Lagoy, 1992; Lara et al., 2023; Kęska and Janicka, 2022) have adapted an idea of toxic equivalent factor (TEF) for overall PAHs toxicity investigation. Nisbet and Lagoy, 1992 have considered benzo[a]pyrene as the reference PAHs (TEF considered as 1.0) to evaluate the overall toxicity of the total PAHs emissions. In the present study, authors have also considered benzo[a] pyrene as the reference PAHs and accordingly the toxic potential of other important PAHs have been adapted as reported by Nisbet and Lagoy, 1992). For example, the TEF values for 1-nitropyrene and chrysene are 0.1 and 0.01 respectively in comparison to the TEF = 1.0 of benzo[a]pyrene (Collins et al., 1998). The composition of these PAHs molecules, in terms of their chemical make-up, is a crucial element in defining the extent of their hazardous potential. Based on this information, the toxicity potential (TP) of a PAHs compound was evaluated using the following expression, (Nisbet and Lagoy, 1992):

TP = TEF x Mass concentration of individual PAHs

Table 3 contains information of TEF and TP for the measured PAHs for comparison with tested fuels.

Fig. 12 shows the individual toxicity of LMW, HMW, and *nitro*-PAHs types of PAHs. It was observed that the toxicity of PAHs is mainly due to HMW and *nitro*-PAH. LMW PAHs exhibit negligible toxicity compared to HMW and *nitro*-PAH. Fig. 13a and b shows the total PAHs, total TP, and total TP/total PAHs for the test fuels. Total PAHs are found to be highest in concentration in the case of diesel (CR17.5), which was followed by B20, E20, and M20 (CR26) as shown in Fig. 13a. Evaluation of toxicity of PAHs (alcohol blends) also showed a similar behaviour of total toxicity reduction. B20 and B50 reduce the total PAHs concentrations by ~33% and ~40% respectively in comparison to the diesel. This fact indicates that B20 was quite effective in reducing the total PAHs concentrations, however, further addition of butanol did not show a significant reduction in the total PAHs emissions. This inference is also true for E20 and E50, as shown in Fig. 13a. This is mainly due to the similar PAHs fraction of B20 and B50 out of total PM emission (Fig. 9) since PM mass is not significantly lowered from B20 to B50. Xiao et al., 2020 have also observed a higher reduction in soot emissions for lower blends in comparison to higher blends of butanol. Moreover, it can be observed that by increasing the blend ratio from 20% to 50% (butanol and ethanol), the total TP value reduced significantly despite having a minor reduction in total PAHs emissions. This is mainly due to the different types of PAHs, in terms of LMW, HMW, and nitro-PAHs distribution, with lower toxicity potential for the higher blending of alcohol fuels (E50 and B50). The lower overall toxicity potential of higher alcohol blend fuels indicates the reduced behaviours of fuel toxicity in terms of PAHs emission which is beneficial from an alternative fuel perspective for alcohols. Fig. 13b shows the total TP/total PAHs as ordinate and fuel blends on abscissa which indicates that E20 has the highest toxicity behaviours which is even higher than diesel, while B50 and E50 showed lower values of total TP/total PAHs in comparison to the other fuels. In the case of alcohol blending with diesel, the formation of PAHs reduces due to the partial replacement of diesel with alcohol molecules during combustion.

4. Conclusions

Methanol-diesel (M20), ethanol-diesel (E20 and E50), and butanol-

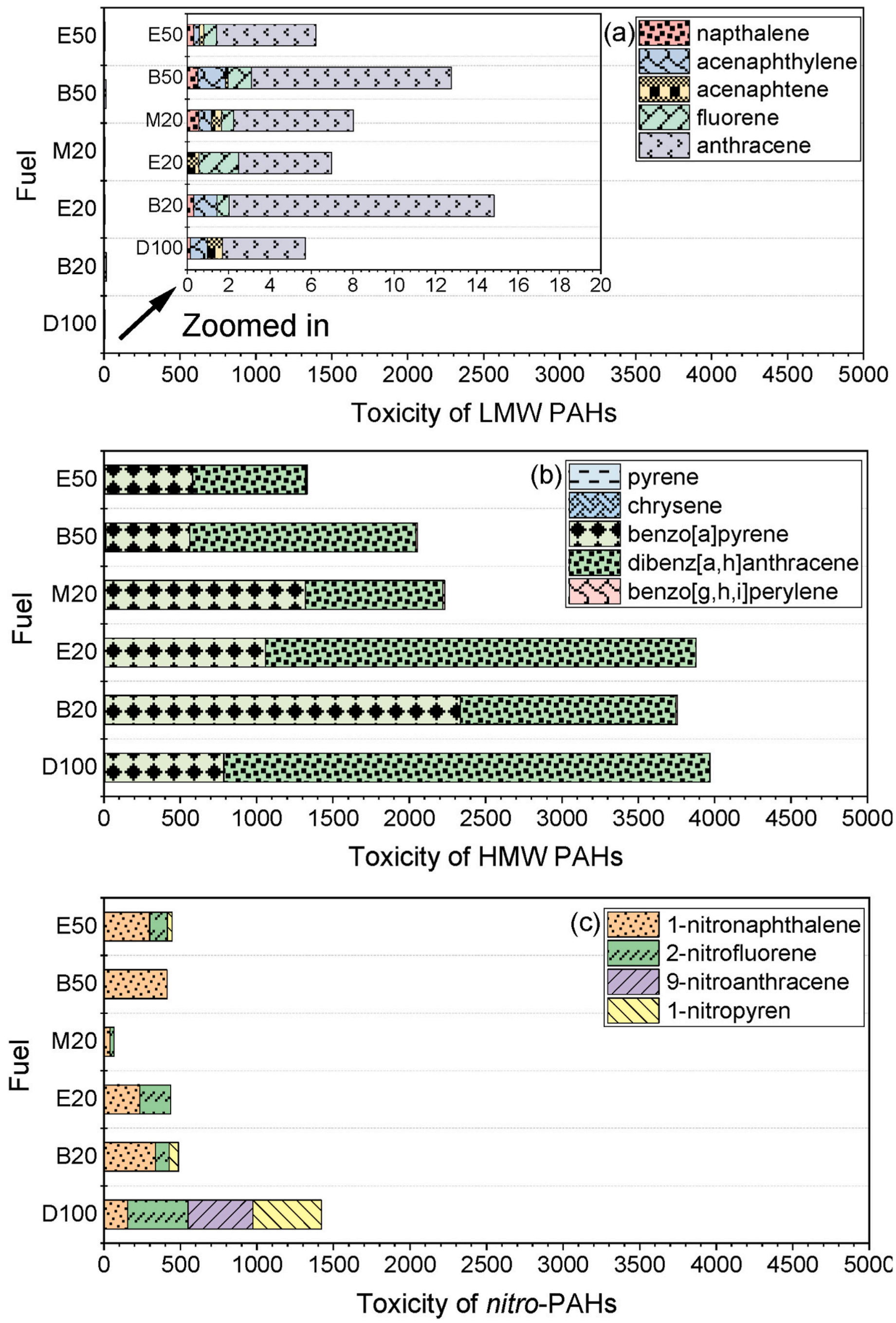

Fig. 12. Toxicity potential of LMW, HMW, and *nitro*-PAHs for diesel (CR17.5) and alcohol-diesel blends (CR26).

diesel (B20 and B50) blends have been tested in a higher compression ratio (CR26) CI engine. Particulate mass and particulate morphology have been measured and analysed. Based on the experiment performed, the following research outcomes are reported below.

- 20% alcohol-diesel blend (methanol, ethanol, and butanol) showed the potential to reduce the PM emission by 30–45% compared to baseline diesel. Alcohols tend to show superior atomization behaviour and thus reduce the overall PM formation during the combustion process.
- For higher alcohol blending ratios (B50 and E50), further reductions in PM emission were not in the relative proportion of alcohol fraction. This depicts that the effectiveness of increasing alcohol fraction diminishes the possibility of proportional PM reduction. E20 and B20 significantly reduced the PM emission by ~38% and ~29%, respectively compared to conventional diesel combustion, while E50 and B50 showed ~54% and ~38% reductions.
- Morphological study of particulate generated from diesel showed fluffy bulk lumps, branched and sticky carbonaceous materials up to 2000 nm, while alcohol blends resulted in discrete smaller sizes in the range of 400–600 nm. SEM images indicate a higher degree of branched agglomerated structure for diesel particulates with high surface area availability compared to alcohol blend generated particulates increasing the probability of absorption/adsorption of volatile organic compounds under the effect of heterogenous nucleation, even before reaching their saturation point.
- A highly agglomerated structure of diesel particulates is observed compared to alcohol blends (methanol, ethanol, and butanol).

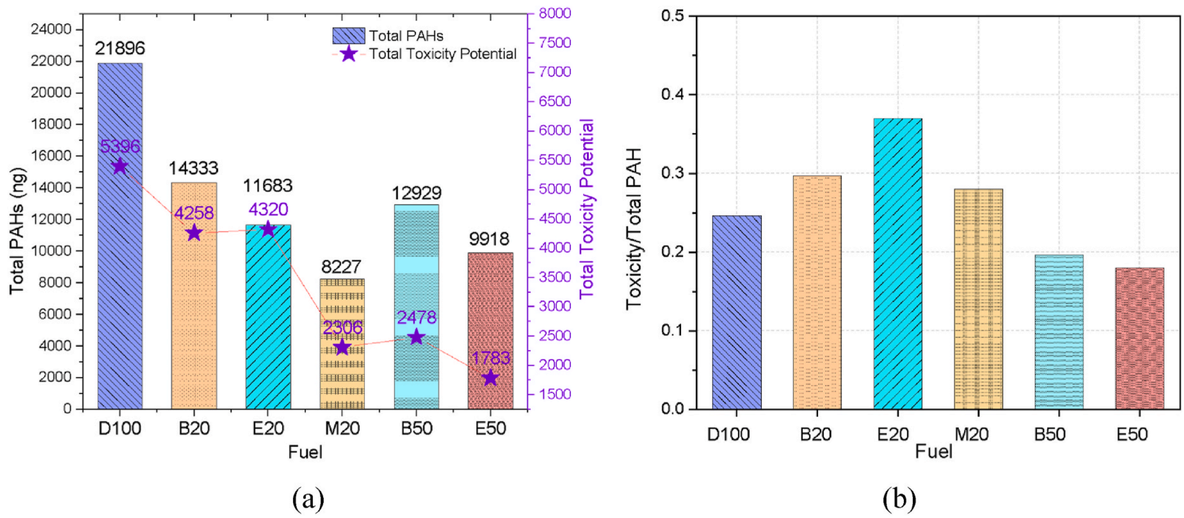

Fig. 13. Total PAHs, TP (a), and TP/total PAHs (b) for diesel (CR17.5) and alcohol-diesel blends (CR26).

Concerning the number of particulates in the given frame of morphological images (diesel and alcohol blends), there are much smaller size of particulates in the case of alcohol blends. This indirectly shows the overall lower particulate mass emission when alcohol blends are used.

- Alcohol blends (methanol, ethanol, and butanol) result in overall lower PAHs emissions than diesel. B20, E20, and M20 fuels indicated a reduction of PAHs of about ~34%, ~46%, and ~62% when compared with diesel. Further increase in alcohol fractions, up to 50% (*v/v*; B50 and E50), showed noticeable, but minor reduction in PAHs emission.
- HMW and *nitro*-PAHs are the main reasons for the overall toxicity of PAHs while the contribution of LMW was found to be negligible. The total toxicity potential B20, E20, M20, B50 and E50 changed by ~21%, ~20%, ~57%, ~54% and ~67% in comparison to diesel. Benzo [a] pyrene and dibenzo-anthracene turned out to be the prominent PAHs emission which also possesses a very high toxic equivalence factor (1.0 and 1.1 respectively).
- E20 showed the highest value of the TP to total PAHs ratio (~0.37) in comparison to diesel (~0.24) and other alcohol blends (methanol, ethanol, and butanol). Although E20 reduces the PAHs emission significantly (~46%), its toxicity per unit mass of PAHs turned out to be the highest among the tested fuels.

Overall, this study highlights that the use of ethanol, methanol, and butanol blended with diesel under the high compression ratio (CR26) operation leads to lower PAHs emission and associated toxicity potential in comparison to the conventional diesel combustion (CR17.5). The morphological study of particulate collected from ethanol, methanol, and butanol blended diesel combustion showed smaller particle size in comparison to the diesel combustion. The utilization of higher fraction of alcohols resulted in a significant reduction in nitro-PAHs and a moderate reduction in HMW PAHs in comparison to diesel combustion. The difficulty of going beyond 50% (*v/v*) blend ratio with higher CR engines can further be investigated by introducing high cetane number additives. It would be interesting to examine the effect of high cetane number additives (ignition improver) with 50% (*v/v*) or higher alcohol blend fractions to improve the ignition quality. Further, other unregulated major emissions such as unburned hydrocarbons, ketone, aldehyde, trace metals etc., can also be studied to evaluate their toxicity potential.

CRediT authorship contribution statement

Tomesh Kumar Sahu: Writing – original draft, Visualization, Validation, Methodology, Investigation, Formal analysis, Data curation, Conceptualization. **Pravesh Chandra Shukla:** Writing – review & editing, Supervision, Resources, Project administration, Formal analysis, Conceptualization. **Arindam Mondal:** Visualization, Validation, Methodology, Investigation, Formal analysis, Data curation. **Satyajit Gupta:** Writing – review & editing, Supervision. **Giacomo Belgiorno:** Writing – review & editing, Visualization, Supervision, Methodology, Formal analysis, Data curation. **Gabriele Di Blasio:** Writing – review & editing, Supervision, Methodology.

Declaration of competing interest

The authors declare that they have no known competing financial interests or personal relationships that could have appeared to influence the work reported in this paper.

Data availability

Data will be made available on request.

Acknowledgement

The authors would like to acknowledge the Department of Mechanical Engineering and Central Instrumentation Facilities of IIT Bhilai for assisting in experiments and analysis for this specific research.

Abbreviations

ATS	Aftertreatment systems
B20	20% butanol with 80% diesel (*v/v*)
B50	50% butanol with 50% diesel (*v/v*)
C/H	Carbon to hydrogen ratio
CI	Compression ignition
CN	Cetane number
CR	Compression ratio
E20	20% ethanol with 80% diesel (*v/v*)
E50	50% ethanol with 50% diesel (*v/v*)
EC	Elemental carbon
EGR	Exhaust gas recirculation
FESEM	Field emission scanning electron microscope
GHG	Greenhouse gases

HCCI	Homogeneous charge compression ignition
HMW	High molecular weight
LCMS	Liquid chromatography with high-resolution mass spectrometer
HVO	Hydrogenated vegetable oil
IARC	International Agency for Research on Cancer
LMW	Low molecular weight
M20	20% methanol with 80% diesel (*v*/*v*)
NIOSH	National Institute for Occupational Safety and Health
OC	Organic carbon
PAHs	Polycyclic aromatic hydrocarbons
PM	Particulate matter
RON	Research octane number
SI	Spark ignition engine
TEF	Toxicity equivalence factor
TP	Toxicity potential

References

Agarwal, A.K., Gupta, T., Kothari, A., 2011. Particulate emissions from biodiesel vs diesel fuelled compression ignition engine. Renew. Sustain. Energy Rev. 15 (6), 3278–3300.
Agarwal, A.K., Srivastava, D.K., Dhar, A., Maurya, R.K., Shukla, P.C., Singh, A.P., 2013a. Effect of fuel injection timing and pressure on combustion, emissions and performance characteristics of a single cylinder diesel engine. Fuel 111, 374–383.
Agarwal, A.K., Gupta, T., Dixit, N., Shukla, P.C., 2013b. Assessment of toxic potential of primary and secondary particulates/aerosols from biodiesel vis-a-vis mineral diesel fuelled engine. Inhal. Toxicol. 25 (6), 325–332.
Agarwal, A.K., Singh, A.P., Gupta, T., Agarwal, R.A., Sharma, N., Rajput, P., et al., 2018. Mutagenicity and cytotoxicity of particulate matter emitted from biodiesel-fueled engines. Environ. Sci. Technol. 52 (24), 14496–14507.
Agarwal, A.K., Singh, A.P., Gupta, T., Agarwal, R.A., Sharma, N., Pandey, S.K., et al., 2020. Toxicity of exhaust particulates and gaseous emissions from gasohol (ethanol blended gasoline)-fuelled spark ignition engines. Environ. Sci. J. Integr. Environ. Res.: Process. Impacts 22 (7), 1540–1553.
Alemahdi, N., Tuner, M., 2020. The effect of 2-ethyl-hexyl nitrate on HCCI combustion properties to compensate ethanol addition to gasoline. Fuel 270, 117569.
Awad, O.I., Mamat, R., Ibrahim, T.K., Hammid, A.T., Yusri, I.M., Hamidi, M.A., et al., 2018. Overview of the oxygenated fuels in spark ignition engine: environmental and performance. Renew. Sustain. Energy Rev. 91, 394–408.
Azami, M.H., Savill, M., 2016. Modelling of spray evaporation and penetration for alternative fuels. Fuel 180, 514–520.
Badawy, T., Xu, H., Li, Y., 2022. Macroscopic spray characteristics of iso-octane, ethanol, gasoline and methanol from a multi-hole injector under flash boiling conditions. Fuel 307, 121820.
Beatrice, C., Di Blasio, G., Belgiorno, G., 2017. Experimental analysis of functional requirements to exceed the 100 kW/l in high-speed light-duty diesel engines. Fuel 207, 591–601.
Belgiorno, G., Di Blasio, G., Shamun, S., Beatrice, C., Tunestål, P., Tunér, M., 2018. Performance and emissions of diesel-gasoline-ethanol blends in a light duty compression ignition engine. Fuel 217, 78–90.
Chang, Y.-C., Lee, W.-J., Lin, S.-L., Wang, L.-C., 2013. Green energy: water-containing acetone–butanol–ethanol diesel blends fueled in diesel engines. Appl. Energy 109, 182–191.
Chen, H., Shi-Jin, S., Jian-Xin, W., 2007. Study on combustion characteristics and PM emission of diesel engines using ester–ethanol–diesel blended fuels. Proc. Combust. Inst. 31 (2), 2981–2989.
Chen, L., Wang, Z., Liu, S., 2017. Study on the effect of diesel blended with n-butanol on particulate matter state characteristics of a small agricultural diesel engine. Bulg. Chem. Commun. 49, 54–58.
Collins, J.F., Brown, J.P., Alexeeff, G.V., Salmon, A.G., 1998. Potency equivalency factors for some polycyclic aromatic hydrocarbons and polycyclic aromatic hydrocarbon derivatives. Regul. Toxicol. Pharmacol. 28 (1), 45–54.
Di Blasio, G., Beatrice, C., Belgiorno, G., Pesce, F.C., Vassallo, A., 2017. Functional requirements to exceed the 100 kW/l milestone for high power density automotive diesel engines. SAE International Journal of Engines 10 (5), 2342–2353.
Di Blasio, G., Ianniello, R., Beatrice, C., Pesce, F.C., Vassallo, A., Belgiorno, G., 2023. Additive manufacturing new piston design and injection strategies for highly efficient and ultra-low emissions combustion in view of 2030 targets. Fuel 346, 128270.
Di Luca, G., Pipicelli, M., Ianniello, R., Belgiorno, G., Di Blasio, G., 2022. Alcohol Fuels in Spark Ignition Engines. Application of Clean Fuels in Combustion Engines. Springer, pp. 33–54.
Eastwood, Peter., 2008. Particulate emissions from vehicles. John Wiley & Sons.
Ghadikolaei, M.A., 2016. Effect of alcohol blend and fumigation on regulated and unregulated emissions of IC engines—a review. Renew. Sustain. Energy Rev. 57, 1440–1495.
Hu, S., Herner, J.D., Robertson, W., Kobayashi, R., Chang, M.C.O., Huang, S-m, et al., 2013. Emissions of polycyclic aromatic hydrocarbons (PAHs) and nitro-PAHs from heavy-duty diesel vehicles with DPF and SCR. J. Air Waste Manag. Assoc. 63 (8), 984–996.
Ianniello, R., Belgiorno, G., Di Luca, G., Beatrice, C., Di Blasio, G., 2021. Ethanol in dual-fuel and blend fueling modes for advanced combustion in compression ignition engines. In: Alcohol as an Alternative Fuel for Internal Combustion Engines. Springer, pp. 5–27.
International Agency for Research on Cancer, 1989. IARC Monographs on the Evaluation of the Carcinogenic Risk of Chemicals to Humans. Distributed for IARC by WHO, Geneva, Switzerland.
Joshi, A., 2023. Year in Review: Progress towards Decarbonizing Transport and Near-Zero Emissions. SAE International.
Kalwar, A., Singh, A.P., Agarwal, A.K., 2020. Utilization of primary alcohols in dual-fuel injection mode in a gasoline direct injection engine. Fuel 276, 118068.
Karavalakis, G., Fontaras, G., Ampatzoglou, D., Kousoulidou, M., Stournas, S., Samaras, Z., et al., 2010. Effects of low concentration biodiesel blends application on modern passenger cars. Part 3: impact on PAH, nitro-PAH, and oxy-PAH emissions. Environ. Pollut. 158 (5), 1584–1594.
Karavalakis, G., Boutsika, V., Stournas, S., Bakeas, E., 2011. Biodiesel emissions profile in modern diesel vehicles. Part 2: effect of biodiesel origin on carbonyl, PAH, nitro-PAH and oxy-PAH emissions. Sci. Total Environ. 409 (4), 738–747.
Kęska, A., Janicka, A., 2022. Evaluation of toxicity of hydrocarbons emitted by Euro 3 and Euro 6 vehicles at idle conditions by means of equivalent toxicity coefficients. Int. J. Engine Res., 14680874221132929
Kim, D., Gautam, M., Gera, D., 2002. Parametric studies on the formation of diesel particulate matter via nucleation and coagulation modes. J. Aerosol Sci. 33 (12), 1609–1621.
Kittelson, D.B., 1998. Engines and nanoparticles: a review. J. Aerosol Sci. 29 (5–6), 575–588.
Lara, S., Villanueva, F., Cabañas, B., Sagrario, S., Aranda, I., Soriano, J.A., et al., 2023. Determination of policyclic aromatic compounds,(PAH, nitro-PAH and oxy-PAH) in soot collected from a diesel engine operating with different fuels. Sci. Total Environ. 900, 165755.
Lei, J., Shen, L., Bi, Y., Chen, H., 2012. A novel emulsifier for ethanol–diesel blends and its effect on performance and emissions of diesel engine. Fuel 93, 305–311.
Li, MD, Wang, Z, Liu, SA, Li, RN, Zhao, Y., 2013. Study on the Particulate Microstructure of Different Oxygenated Fuels. 726. Trans Tech Publ 1950–1953.
Malmborg, V.B., Eriksson, A.C., Shen, M., Nilsson, P., Gallo, Y., Waldheim, B., et al., 2017. Evolution of in-cylinder diesel engine soot and emission characteristics investigated with online aerosol mass spectrometry. Environ. Sci. Technol. 51 (3), 1876–1885.
Maricq, M.M., 2007. Chemical characterization of particulate emissions from diesel engines: a review. J. Aerosol Sci. 38 (11), 1079–1118.
McCaffery, C., Zhu, H., Sabbir Ahmed, C.M., Canchola, A., Chen, J.Y., Li, C., et al., 2022. Effects of hydrogenated vegetable oil (HVO) and HVO/biodiesel blends on the physicochemical and toxicological properties of emissions from an off-road heavy-duty diesel engine. Fuel 323, 124283.
Medina, C., Santos-Martinez, M.J., Radomski, A., Corrigan, O.I., Radomski, M.W., 2007. Nanoparticles: pharmacological and toxicological significance. Br. J. Pharmacol. 150 (5), 552–558.
Merritt, P.M., Ulmet, V., McCormick, R.L., Mitchell, W.E., Baumgard, K.J., 2005. Regulated and unregulated exhaust emissions comparison for three tier II non-road diesel engines operating on ethanol-diesel blends. SAE Trans. 1111–1122.
Nisbet, I.C.T., Lagoy, P.K., 1992. Toxic equivalency factors (TEFs) for polycyclic aromatic hydrocarbons (PAHs). Regul. Toxicol. Pharmacol. 16 (3), 290–300.
Nord, K., Haupt, D., Ahlvik, P., Egebäck, K.-E., 2004. Particulate Emissions from an Ethanol Fueled Heavy-Duty Diesel Engine Equipped with EGR, Catalyst and DPF. SAE Technical Paper.
Nour, M., Attia, A.M.A., Nada, S.A., 2019a. Improvement of CI engine combustion and performance running on ternary blends of higher alcohol (Pentanol and Octanol)/hydrous ethanol/diesel. Fuel 251, 10–22.
Nour, M., Attia, A.M.A., Nada, S.A., 2019b. Combustion, performance and emission analysis of diesel engine fuelled by higher alcohols (butanol, octanol and heptanol)/diesel blends. Energy Convers. Manag. 185, 313–329.
Otsuki, T., Holian, A., Di Gioacchino, M., 2014. Immunological Effects of Environmental Factors: Focus on the Fibrous and Particulated Materials. Hindawi, p. 2014.
Paim, J.N., Santos, A.G., Araujo, R.G.O., Nascimento, M.M., De Andrade, J.B., Guarieiro, L.L., 2023. Emissions of PAHs, nitro-PAHs and quinones (Oxy-PAHs) associated to PM1.0 and PM2.5 emitted by a diesel engine fueled with diesel-biodiesel-ethanol blends. Atmosphere 14.
Pierdominici, M., Maselli, A., Cecchetti, S., Tinari, A., Mastrofrancesco, A., Alfè, M., et al., 2014. Diesel exhaust particle exposure in vitro impacts T lymphocyte phenotype and function. Part. Fibre Toxicol. 11, 74.
Rajeev, P., Shukla, P.C., Singh, G.K., Das, D., Gupta, T., 2023. Assessment of entrainment of key PAHs emanating from major combustion sources into the ambient air. Fuel 347, 128430.
Rana, S., Saxena, M.R., Maurya, R.K., 2022. A review on morphology, nanostructure, chemical composition, and number concentration of diesel particulate emissions. Environ. Sci. Pollut. Control Ser. 29 (11), 15432–15489.
Ravindra, K., Sokhi, R., Van Grieken, R., 2008. Atmospheric polycyclic aromatic hydrocarbons: source attribution, emission factors and regulation. Atmos. Environ. 42 (13), 2895–2921.
Ribeiro, C.B., Rodella, F.H.C., Hoinaski, L., 2022. Regulating light-duty vehicle emissions: an overview of US, EU, China and Brazil programs and its effect on air quality. Clean Technol. Environ. Policy 1–12.

Ruiz, F.A., Cadrazco, M., López, A.F., Sanchez-Valdepeñas, J., Agudelo, J.R., 2015. Impact of dual-fuel combustion with n-butanol or hydrous ethanol on the oxidation reactivity and nanostructure of diesel particulate matter. Fuel 161, 18–25.

Sahu, T.K., Shukla, P.C., 2022a. Combustion and Emission Characteristics of Butanol-Diesel Blend (B15) Doped with Diethyl Ether, Diglyme and Ethyl Diglyme in a CRDI Diesel Engine. SAE Technical Paper.

Sahu, T.K., Shukla, P.C., 2022b. Effect of inherent oxygen mass fraction of alcohol blends with diesel on combustion and emission parameters. Environ. Prog. Sustain. Energy, e14030 n/a(n/a).

Sahu, T.K., Shukla, P.C., Belgiorno, G., Maurya, R.K., 2022a. Alcohols as alternative fuels in compression ignition engines for sustainable transportation: a review. Energy Sources, Part A Recovery, Util. Environ. Eff. 44 (4), 8736–8759.

Sahu, T.K., Sahu, V.K., Mondal, A., Shukla, P.C., Gupta, S., Sarkar, S., 2022b. Investigation of sugar extraction capability from rice paddy straw for potential use of bioethanol production towards energy security. Energy Sources, Part A Recovery, Util. Environ. Eff. 44 (1), 272–286.

Shamun, S., Haşimoğlu, C., Murcak, A., Andersson, Ö., Tunér, M., Tunestål, P., 2017. Experimental investigation of methanol compression ignition in a high compression ratio HD engine using a Box-Behnken design. Fuel 209, 624–633.

Shamun, S., Belgiorno, G., Di Blasio, G., Beatrice, C., Tunér, M., Tunestål, P., 2018. Performance and emissions of diesel-biodiesel-ethanol blends in a light duty compression ignition engine. Appl. Therm. Eng. 145, 444–452.

Shanmugam, R., Murugesan, P., Guye, G.G., Duraisamy, B., 2021. Effect of additives on the stability of ethanol-diesel blends for IC engine application. Environ. Sci. Pollut. Control Ser. 28, 12153–12167.

Shukla, P.C., Gupta, T., Agarwal, A.K., 2014. A comparative morphological study of primary and aged particles emitted from a biodiesel (B20) vis-à;-vis diesel fuelled CRDI engine. Aerosol Air Qual. Res. 14 (3), 934–942.

Shukla, P.C., Gupta, T., Labhsetwar, N.K., Agarwal, A.K., 2017. Trace metals and ions in particulates emitted by biodiesel fuelled engine. Fuel 188, 603–609.

Shukla, P.C., Gupta, T., Agarwal, A.K., 2018. Techniques to control emissions from a diesel engine. Air pollution and control 57–72.

Singh, G.N., Bharj, R.S., 2019. Study of physical-chemical properties for 2nd generation ethanol-blended diesel fuel in India. Sustainable Chemistry and Pharmacy 12, 100130.

Singh, S., Kulshrestha, M.J., Rani, N., Kumar, K., Sharma, C., Aswal, D.K., 2023. An overview of vehicular emission standards. Mapan 38 (1), 241–263.

Song, C.-L., Zhou, Y.-C., Huang, R.-J., Wang, Y.-Q., Huang, Q.-F., Lü, G., et al., 2007. Influence of ethanol–diesel blended fuels on diesel exhaust emissions and mutagenic and genotoxic activities of particulate extracts. J. Hazard Mater. 149 (2), 355–363.

Tse, H., Leung, C.W., Cheung, C.S., 2015. Investigation on the combustion characteristics and particulate emissions from a diesel engine fueled with diesel-biodiesel-ethanol blends. Energy 83, 343–350.

Tuner, M., 2016. Review and Benchmarking of Alternative Fuels in Conventional and Advanced Engine Concepts with Emphasis on Efficiency, CO_2, and Regulated Emissions. SAE International.

Van Setten, B.A.A.L., Makkee, M., Moulijn, J.A., 2001. Science and technology of catalytic diesel particulate filters. Catal. Rev. 43 (4), 489–564.

Verhelst, S., Turner, J.W.G., Sileghem, L., Vancoillie, J., 2019. Methanol as a fuel for internal combustion engines. Prog. Energy Combust. Sci. 70, 43–88.

Wang, Y., Liu, H., Lee, C.-F.F., 2016. Particulate matter emission characteristics of diesel engines with biodiesel or biodiesel blending: a review. Renew. Sustain. Energy Rev. 64, 569–581.

Xiao, H., Guo, F., Wang, R., Yang, X., Li, S., Ruan, J., 2020. Combustion performance and emission characteristics of diesel engine fueled with iso-butanol/biodiesel blends. Fuel 268, 117387.

Xu, J., Lyu, Y., Zhuo, J., Xu, Y., Zhou, Z., Yao, Q., 2021. Formation and emission characteristics of VOCs from a coal-fired power plant. Chin. J. Chem. Eng. 35, 256–264.

Xu, C., Zhuang, Y., Qian, Y., Cho, H., 2022. Effect on the performance and emissions of methanol/diesel dual-fuel engine with different methanol injection positions. Fuel 307, 121868.

Yesilyurt, M.K., Aydin, M., Yilbasi, Z., Arslan, M., 2020. Investigation on the structural effects of the addition of alcohols having various chain lengths into the vegetable oil-biodiesel-diesel fuel blends: an attempt for improving the performance, combustion, and exhaust emission characteristics of a compression ignition engine. Fuel 269, 117455.

Yilmaz, N., Davis, S.M., 2016. Polycyclic aromatic hydrocarbon (PAH) formation in a diesel engine fueled with diesel, biodiesel and biodiesel/n-butanol blends. Fuel 181, 729–740.

Yilmaz, N., Davis, S.M., 2022a. Formation of polycyclic aromatic hydrocarbons and regulated emissions from biodiesel and n-butanol blends containing water. J. Hazard Mater. 437, 129360.

Yilmaz, N., Davis, S.M., 2022b. Diesel blends with high concentrations of biodiesel and n-butanol: effects on regulated pollutants and polycyclic aromatic hydrocarbons. Process Saf. Environ. Protect. 166, 430–439.

Yilmaz, N., Donaldson, A.B., 2005. Examination of Causes of Wetstacking in Diesel Engines. SAE Technical Paper.

Yilmaz, N., Vigil, F.M., Donaldson, B., 2022. Fuel effects on PAH formation, toxicity and regulated pollutants: detailed comparison of biodiesel blends with propanol, butanol and pentanol. Sci. Total Environ. 849, 157839.

Yuan, Z., Li, G., Hegg, E.L., 2018. Enhancement of sugar recovery and ethanol production from wheat straw through alkaline pre-extraction followed by steam pretreatment. Bioresour. Technol. 266, 194–202.

Yusuf, A.A., Yusuf, D.A., Jie, Z., Bello, T.Y., Tambaya, M., Abdullahi, B., et al., 2022. Influence of waste oil-biodiesel on toxic pollutants from marine engine coupled with emission reduction measures at various loads. Atmos. Pollut. Res. 13 (1), 101258.

Zhang, Z.H., Tsang, K.S., Cheung, C.S., Chan, T.L., Yao, C.D., 2011. Effect of fumigation methanol and ethanol on the gaseous and particulate emissions of a direct-injection diesel engine. Atmos. Environ. 45 (11), 2001–2008.

Zhang, W., Cui, M., Yao, B., Nour, M., Li, X., Xu, M., 2023. Investigating the relationship between butanol molecular structure and combustion performance in an optical SIDI engine. Energy Convers. Manag. X 20, 100455.

Zhao, W., Yan, J., Gao, S., Lee, T.H., Li, X., 2022. The combustion and emission characteristics of a common-rail diesel engine fueled with diesel and higher alcohols blends with a high blend ratio. Energy 261, 124972.